Desalination and Water Treatment
www.deswater.com
doi: 10.5004/dwt.2021.26477

209 (2021) 91–104
January

Kinetic and isotherm study of Cr(VI) biosorption from industrial effluents by biomass of dried sludge

Fatemeh Kariminejad[a], Samira Baghchevan Ghadimi[b], Farhad Rahmani[c], Mohsen Haghighi[d], Rojiar Akbari Sene[c,*], Mohammad Ali Zazouli[e,*], Elham Sadat Heydari[a]

[a]*Department of Environmental Health Engineering, School of Health, Mashhad University of Medical Sciences, Mashhad, Iran, emails: Kariminezhad136618@gmail.com (F. Kariminejad), heidarielham72@gmail.com (E.S. Heydari)*
[b]*Faculty of Chemical Engineering, Sahand University of Technology, Tabriz, Iran, email: S.bagchevan91@yahoo.com (S.B. Ghadimi)*
[c]*Department of Chemical Engineering, Faculty of Engineering, University of Kurdistan, Sanandaj, Iran, emails: F.rahmanichiyane@uok.ac.ir (F. Rahmani), r.akbari@uok.ac.ir (R. Akbari Sene)*
[d]*Faculty of Health, Kashan University of Medical Sciences, Kashan, Iran, email: mohsenhaghighi087@gmail.com (M. Haghighi)*
[e]*Department of Environmental Health Engineering, Health Sciences Research Center, Faculty of Health, Mazandaran University of Medical Sciences, Sari, Iran, email: Zazoli49@yahoo.com (M.A. Zazouli)*

Received 29 September 2019; Accepted 24 August 2020

ABSTRACT

In the present study, biosorption of Cr(VI) from synthetic and real industrial effluents by biomass of dried sludge as an effective and eco-friendly biosorbent was evaluated. The fresh and spent biosorbent was characterized by scanning electron microscopy, Fourier-transform infrared spectroscopy, energy-dispersive X-ray, and Brunauer–Emmett–Teller (BET) techniques. These structural and morphological characterizations designated that prepared biosorbent has potent adsorptive functional groups (oxygen-containing functional groups), heterogeneous, and a porous surface. Moreover, the BET result indicated that the biomass of dried sludge with a surface area of 8.79 m^2/g can provide a suitable surface for the biosorption of Cr(VI). The key experimental parameters were investigated to examine their feasibility in the maximum removal of Cr(VI). Furthermore, kinetic models were assessed, providing the best fitting for the experimental data. For evaluating the mechanism of the biosorption process, isotherms were also conducted under optimum adsorption conditions. The post characterization results confirmed the adsorption of Cr species onto the sludge surface. The maximum biosorption efficiency of Cr(VI) was found at 83.96% and at initial Cr(VI) concentration of 50 mg/L, time of 100 min, biosorbent dosage of 8 g/L, and pH of 5. Kinetic study showed the biosorption process follows the pseudo-second-order kinetic model (R^2 = 0.9973 and k_2 = 1.8 × 10^{-3} g/mg min), which suggests the adsorption process involves a chemisorption mechanism. The half-life of Cr(VI) removal in the biosorption process was 0.6 h. Also, the isotherm study revealed that Cr(VI) biosorption process was best fitted with the Redlich–Peterson model (R^2 = 0.9993) with a maximum Cr ion sorption capacity of 9.082 mg/g. This result confirms that chromium removal occurs on a biosorbent with the homogenous surface by monolayer adsorption. Besides, the Gibbs free energy ($\Delta G°$) value obtained from thermodynamic equilibrium reaffirmed that the prepared biosorbent possesses a large capacity for biosorption of Cr(VI). Finally, the results promulgated that biomass of dried sludge can be applied as an effective and practical biosorbent for the removal of Cr(VI) from industrial wastewater.

Keywords: Biosorption; Industrial wastewater; Dried sludge; Isotherm; Chromium

* Corresponding authors.

1. Introduction

One of the environmental challenges and concerns is the entry of heavy metals into the environment through the release of various types of industrial wastewater and effluents, increasing owing to the expansion of industries [1]. If they enter the environment, they will cause the environmental consequences for living organisms and human health due to their sustainability and the high transfer power in water resources [2]. Heavy metals classify into three main subgroups: toxic metals (Hg, Cr, Pb, Zn, Cu, Ni, Cd, As, Co, Sn, etc.), precious metals (Pd, Pt, Ag, Au, Ru, etc.) and radionuclide (U, Th, Ra, Am). According to the World Health Organization's (WHO) list of 10 chemicals by major public concern, cadmium, mercury, lead, and arsenic are highlighted because of their high water solubility, toxicity, and carcinogenesis [3–6]. Based on this classification, hexavalent chromium (Cr(VI)) is one of the major environmental concerns because of its potential for skin allergies, carcinogenicity, the ability to change the nature of DNA and high toxicity [7,8], and it is classified as a priority pollutant by the United States Environmental Protection Agency (EPA) in terms of toxicity. Hence, its maximum permitted level for drinking water has been determined by 0.1 mg/L [9]. Cr(VI) is expansively used in various industries like leather manufacturing, batteries, paper production, fertilizer industries, alloy mills, and steel manufacturing plants, washing and polishing metals, tannery, refiners, and especially electroplating industries [10,11]. Considering the mentioned issues in the area of environmental problems and existing limitations, the treatment of wastewater released from various industries containing a substantial amount of Cr(VI) is absolutely necessary prior to discharge into the environment and water resources [12]. Therefore, several methods are used to remove Cr(VI) from industrial effluents and sewage, including chemical methods [13], chemical precipitation [14], electrocoagulation [15], membrane processes [16], nanoparticles and nanotubes [17], and biological processes [18]. However, most of these methods require high costs, especially at the actual and industrial scale; and in most cases, they are not able to eliminate the acceptable percentage of the pollutant [19,20]. Moreover, biological processes, which are relatively more practical and applicable to different industries, are less effective due to the toxic effect of Cr(VI) and disturbance in the metabolic activity of microorganisms [21].

Among these methods, adsorption is a common method in the removal of heavy metals for various types of wastewater due to its special characteristics such as: cost-effectively, design simplicity and easy operation [4]. In recent years, among the various studies conducted in the field of adsorption method, the biosorption process has been considered as one of the most effective methods for the removal of heavy metals [22,23]. Biosorbents with high biosorption capacity and low operational costs are the most suitable alternatives for conventional adsorbents. In the biosorption process, both groups of microorganisms (biologically active and inactive) are able to adsorb heavy metal ions [24]. Activated sludge by various functional groups such as carboxylic acid, carboxyl, and amine groups is an effective and eco-friendly biosorbent for biosorption of metal ions [25]. Numerous studies have shown that, in addition to these groups, other functional groups such as aldehyde, phosphoryl, and hydroxyl in the activated sludge composition are considered as the main functional groups in the removal of metal ions in aqueous media [26]. Furthermore, the formation of these functional groups in active sludge can be increased by pretreatment methods such as heating, autoclaving, and acidifying [27].

A large number of studies have been performed to evaluate the efficiency and performance of various biosorbent for biosorption of heavy metals, including biosorption of chromium on barley hull and barley hull ash [28], biosorption of Cd(II) and Cr(VI) by mesocarps of orange and sour orange [29], biosorption of heavy metals from industrial effluents by microalgae [30], and resistant bacterium [31]. Nonetheless, to our best knowledge, there are limited studies about the removal of Cr(VI) from synthetic and real sewage samples taken from electroplating industries using dried activated sludge. Therefore, the present work investigated the biosorption efficiency and behavior of dried activated sludge derived from the return line sludge of sedimentation tank in case of hexavalent chromium. The desired adsorbent was collected and prepared as low-cost locally available adsorbents by heating and drying methods and none activators were used in the preparation process. Moreover, the physicochemical characterization of processed biosorbent was done by different types of techniques scanning electron microscopy-energy-dispersive X-ray (SEM-EDX), Brunauer–Emmett–Teller (BET), and Fourier-transform infrared spectroscopy (FTIR). The effect of various operating parameters (Cr(VI) initial concentration, biosorbent dose, pH, time) on the biosorption process was investigated in a batch reactor. Furthermore, the rate of kinetics and equilibrium parameters was determined. Biosorption isotherm models and thermodynamic parameters were also appraised to know biosorption behavior. Adsorption performance and possible mechanisms of the Cr(VI) biosorbent were investigated in detail. Finally, the efficiency of activated sludge biosorbent under optimum conditions was evaluated on the removal of Cr(VI) from the real sewage samples regarding electroplating industries.

2. Materials and methods

2.1. Chemicals

To adjust the pH, 0.5 N NaOH and HCl solutions were applied. Preparation of standard chromium solutions was carried out using potassium dichromate ($K_2Cr_2O_7$). Standard solutions were made in the range of 5–200 mg/L. All solutions were prepared by double distilled water (EC < 5). Chemicals with analytic grade were provided from Merck Co., Germany.

2.2. Preparation of biosorbent

The sludge was provided from the return sludge of the secondary sedimentation tank of the municipal wastewater treatment plant as well as was characterized by various methods (Table 1). The heating and drying method was used for the preparation of the sludge. Accordingly, the

Table 1
Summary of characteristics of dried activated sludge

Parameter	Concentration
Sludge volume index (mg/L)	89 ± 11
Volatile suspended solids/mixed liquor suspended solids (%)	76 ± 4
Floc size (μm)	315 ± 3
Total dry solids (TS), %	6.5
Volatile solids (% of TS)	75
pH	6.5

sludge was dried in 105°C for 48 h until reaching its constant weight, and it dried, crushed, and sieved into particle size using sieve particles (50–60 mesh). To measure Cr(VI) in primary sludge, acid digestion by HNO_3 and H_2O_2 solutions was used according to EPA Method 3050B [32]. The samples digested after passing through the Whatman filter paper and the Cr(VI) concentration was determined by atomic absorption device (model: Agilent 55B AA, USA). Since Cr(VI) concentration in three stages of measurement was less than 0.6 ± 0.3 mg/g of sludge, this concentration was discarded at the next stages.

2.3. Preparation of simulated industrial wastewater

The real samples were collected from the wastewater treatment plant of the electroplating industry in Mashhad, and analyzed (Table 2). The Cr(VI) concentration in the effluent was measured to be in the range of 13.16 to 89.85 mg/L. The pH of this wastewater was also recorded at a range of 6.6–7.6. Therefore, synthetic effluent using $K_2Cr_2O_7$ salt was prepared at a concentration of 50 to 300 mg/L.

2.4. Determination of biosorbent characteristics

The surface morphology of the biomaterial was studied by SEM analyzer (HITACHI S-4160, Japan) with an acceleration voltage of 15 kV. For the elemental analysis of the biosorbent surface, EDX analysis was conducted on the same field-emission scanning electron microscopy (FESEM) instrument equipped with a BSE detector. The specific surface area of samples was determined by the BET method using N_2 adsorption–desorption isotherms via MicrotracBEL analyzer (BELSORP-mini II, Japan). To characterize surface functional groups, FTIR spectra collected on KBr-diluted palletized samples using a UNICAM 4600 spectrophotometer in the wave-number range of 400–4,000 cm^{-1}.

Also, to validate the biosorbent surface charge, the pH of the point of zero charges (pH_{PZC}) was measured. For this purpose, 0.01 N NaCl was used as an electrolyte and 0.1 M NaOH and HCl solutions used as controllers. 30 mL of the electrolytic solution along with 0.5 g of biosorbent poured in 6 Erlenmeyer flasks and the pH adjusted in a range of 2–12, and the flasks were shaken at 120 rpm for 48 h. The biosorbent was then separated by a filter and the final pH recorded. The pH_{PZC} of the biosorbent was measured by drawing a curve ΔpH (pH initial – pH final) vs. pH initial [33].

Table 2
Characteristics of real electroplating industries effluent samples

SI. No.	Parameters	Concentration
1	Total dissolved solids	13.16–89.85 (mg/L)
2	Oil & grease	8–11 (mg/L)
3	Temperature	23°C–25°C
4	Hexavalent chromium	13.16–89.85 (mg/L)
5	Nickel	2.4–4.5 (mg/L)
6	Copper	12.94–14.67 (mg/L)
7	Cadmium	0.03–1.2 (mg/L)
8	Total residual chlorine	15.58–16.27 (mg/L)
9	Chemical oxygen demand	90.81–219.91 (mg/L)
10	Biochemical oxygen demand	29.71–101.61 (mg/L)
11	Color	34.05–113.58 (TCU)

2.5. Batch experiments procedure

The experiments were performed using a 500 mL container in the batch system and at laboratory temperature. To mix, the shaker at a speed of 100 rpm was used. The experiments carried out using the optimization method and the effect of parameters affecting the Cr(VI) removal efficiency, that is, initial concentration of Cr(VI) (50, 100, 150, 200, 250 and 300 mg/L), time (10, 20, 60, 80, 100, 120 min), biosorbent dosage (2, 4, 6, 8, 10 g/L) and pH (3, 5, 7, 9, 11) were investigated. To carry out experiments, the effect of time was investigated initially under constant conditions (initial Cr(VI) concentration of 50 mg/L, biosorbent dosage of 2 g/L and pH of 5). After determining the optimal time, the same procedure was used to determine the optimal biosorbent dosage (at the optimal time, the initial Cr(VI) concentration of 50 mg/L and pH of 5), the initial Cr(VI) concentration (at the optimal time, biosorbent dose and pH of 5) and to estimate pH (at optimal initial concentration, biosorbent time and dose). At the end of the experiments, the samples were filtrated and kept at pH less than 2 (using concentrated HNO_3).

2.6. Determination of biosorption isotherm

The biosorption isotherms are very important from the theoretical and practical points of view in processes. In particular, it is essential in adsorption and biosorption processes for determining the effective design of systems and biosorbent capacity and also, mathematical modeling of the process [34]. The abilities of six widely used isotherms, that is, Langmuir, Freundlich, Temkin, Scatchard, Dubinin–Radushkevich, and Redlich–Peterson isotherms, to model the equilibrium adsorption data were examined.

The linear form of the Langmuir equation is as follows:

$$\frac{C_e}{q_e} = \frac{1}{K_L q_m} + \frac{C_e}{q_m} \tag{1}$$

In this equation, q_e is the amount of adsorbed adsorbate per unit mass of the adsorbent (mg/g), C_e is the equilibrium concentration of the adsorbate in the solution after the biosorption process (mg/L), q_m is the biosorption capacity and

K_L is Langmuir constant, which is obtained by plotting C_e/q_e against C_e.

The linearized form of the Freundlich equation is also represented by the below equation:

$$\log q_e = \log K_F + \frac{1}{n}\log c_e \tag{2}$$

In this equation, q_e is the amount of substance adsorbed per mass of adsorbent (mg/g), C_e is the equilibrium concentration of adsorbate in the solution after the biosorption process (mg/L), n and K_F, are representative of the biosorption rate and biosorption capacity, respectively which is derived from drawing $\log q_e$ vs. $\log C_e$ [9].

The experimental data were also considered to the Temkin isotherm model in which during adsorbent-adsorbate interaction, the heat of adsorption of all molecules in layer decreases linearly with coverage. The Temkin isotherm model can be expressed in a linear form by Eqs. (3) and (4):

$$q_e = B\ln A_T + B\ln C_e \tag{3}$$

$$B = \frac{RT}{b} \tag{4}$$

In this equation, q_e is the amount of Cr(VI) absorbed per unit mass of adsorbent (mg/g), A_T is Temkin isotherm equilibrium constant related to its binding energy (L/g), C_e is the equilibrium concentration of metal ions (mg/g), B is constant related to the heat of adsorption (J/mol), R is the universal gas constant (8.314 J/mol K), T is the absolute temperature (K) and b is Temkin isotherm constant, which shows the adsorption potential of the adsorbent. The constants A_T and $B = RT/b$ were calculated from the slope and intercept of the Temkin plot of q_e against $\ln C_e$.

Scatchard isotherm is a widely used model for investigating the type of interaction taking part in a particular adsorption process. The type of adsorbate–biosorbent interaction depends on the shape of the Scatchard plot. When the Scatchard isotherm plot is linear with a negative slope, interaction between chromium ions and adsorption sites follows the Langmuir model but if this plot shows a deviation from linearity, the interaction type corresponds to the analysis of adsorption data in terms of the Freundlich isotherm model. The Scatchard isotherm model in a linear form is expressed as follows:

$$\frac{q_e}{C_e} = Q_s K_s - q_e K_s \tag{5}$$

where K_s (L/mg) and Q_s (mg/g) are the adsorption isotherm parameters of Scatchard and are calculated from the slope and intercept of the Scatchard plot of q_e/C_e against q_e, respectively.

The Dubinin–Radushkevich isotherm is another two parameters isotherm model equation, which can be expressed in a linear form as follows:

$$\ln q_e = \ln q_m - \beta\varepsilon^2 \tag{6}$$

$$\varepsilon = RT\ln\left(1+\frac{1}{C_e}\right) \tag{7}$$

$$E = \frac{1}{\sqrt{2\beta}} \tag{8}$$

In this equations, q_m is the theoretical maximum adsorption capacity of adsorbent (mg/g), β is the constant related to adsorption energy (mol^2/J^2), R is the universal gas constant (8.314 J/mol K) and T is the temperature (K) and ε is a polanyi potential (J/mol) which is shown by Eq. (7) and E is the mean energy of sorption (J/mol) which is presented by Eq. (8). Radushkevich isotherm is useful to study the sorption properties and establish the dominant mechanism in terms of ion exchange or physical adsorption based on the value of E. The values of E between 8 and 16 kJ/mol confirm that the adsorption is of chemical type possibly in terms of the ion exchange process and E values less than 8 kJ/mol confirm the physical nature of adsorption [35–37].

The slope and intercept of a graph plotted between $\ln q_e$ and ε^2 gives the values of β and q_m, respectively. Redlich–Peterson isotherm is a three-parameter isotherm model that represents the characteristics of both Langmuir and Freundlich isotherms. Therefore, the mechanism of adsorption is a mix and does not follow the ideal monolayer adsorption. The model behaves like the Freundlich at high adsorbate concentrations and closes to Henry's law at low concentrations [18]. The Redlich–Peterson isotherm equation is generally expressed as follows:

$$q_e = \frac{AC_e}{1+BC_e^g} \tag{9}$$

where A, B and g which are the parameters of Redlich–Peterson isotherm can be obtained from a plot between $\left(A\frac{C_e}{q_e}-1\right)$ and $\ln C_e$. However, this is impossible since it contains three parameters. Thus, a trial and error procedure is adopted to estimate the parameter A by maximizing the R^2 value using the Solver add-in, Microsoft Excel. For conducting experiments, initial Cr(VI) concentrations including 50, 100, 150, 200, 250, and 300 mg/L were investigated under optimal conditions of other parameters.

2.7. Determination of the kinetics

The kinetic equations evaluate to describe the behavior of the transfer of the adsorbate molecules and the factors affecting the rate of the biosorption process. In this study, the pseudo-first-order, pseudo-second-order kinetic, and intraparticle diffusion models under optimum conditions at different times investigated for the Cr(VI) biosorption. The linear form of the first-order kinetic equation is presented in Eq. (10).

$$\log\left(q_e - q_t\right) = \log q_e - \left(\frac{k_1 t}{2.303}\right) \tag{10}$$

In this equation, q_e and q_t are biosorption capacities in equilibrium and time t, respectively, and k_1 is the pseudo-first-order coefficient.

The pseudo-second-order kinetic indicates that the chemisorption is a rate-limiting step and controls the biosorption processes. The equation of the pseudo-second-order model is based on solid-phase biosorption, and q_e and k_2 are calculated through plotting t/q_e vs. t. The linear form of the model is expressed in Eq. (11).

$$\frac{t}{q_e} = \frac{1}{(k_2 q_e^2)} + \left(\frac{1}{q_e}\right)t \tag{11}$$

Furthermore, the equation for the intraparticle diffusion model is calculated by the following equation Eq. (12) [38]:

$$q_t = k\,t^{0.5} + c \tag{12}$$

The biosorption rate of half of the contaminants ($t_{1/2}$) in the solution was also calculated according to the following equation Eq. (13) [39]:

$$t_{\frac{1}{2}} = \frac{1}{k_2 q_e} \tag{13}$$

2.8. Statistical analyzes

Statistical analysis of data was analyzed by Excel 2016 and SPSS 16 software. Kolmogorov–Smirnov test was used to check the normality of data and the significance level was considered as 0.05.

3. Results and discussion

3.1. Surface characteristics of prepared biosorbent

SEM images and EDX spectrums of prepared biosorbent before and after adsorption of Cr(VI) ions have been shown in Fig. 1. As can be seen, the prepared adsorbent before adsorption has a heterogeneous and porous surface. In contrast, a relatively nonporous surface can be realized from the SEM image of the spent biosorbent which is attributed to the pore blockage and adsorbent surface converge by adsorbate. By comparing the EDX spectrum of fresh and spent adsorbent, it can be concluded that Cr(VI) is adsorbed onto the sludge surface.

As well known, the specific surface area of the adsorbent is one of the main factors that affects the adsorption process. In this regard, the specific surface area of the adsorbent before and after adsorption was estimated by the BET technique and 8.79 and 3.85 m^2/g was calculated, respectively.

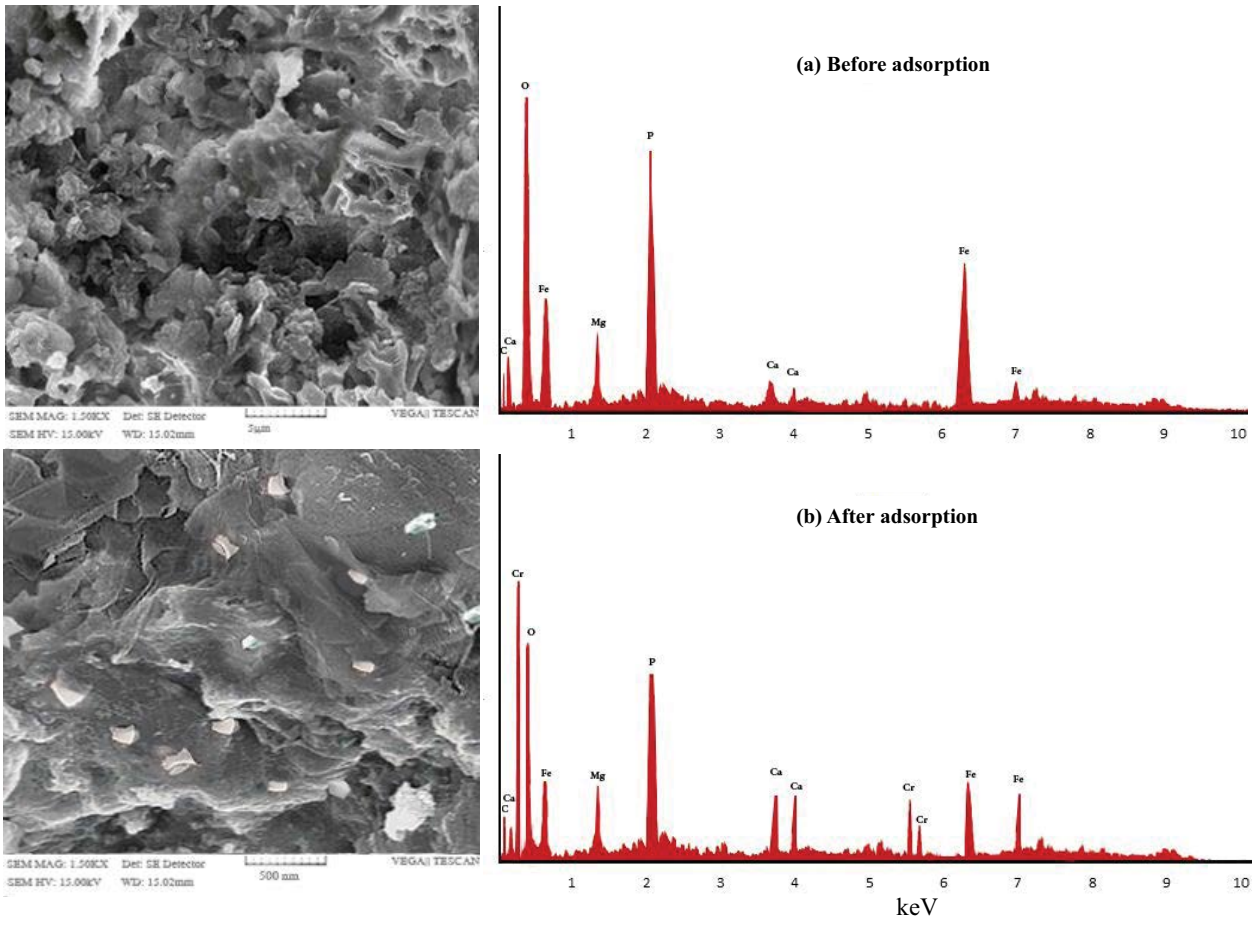

Fig. 1. SEM micrograph and EDX spectrum of the adsorbent surface (a) before and (b) after Cr adsorption.

The fresh adsorbent exhibited a relatively high surface area which can facilities the adsorption process. The examination of the BET data reveals that after exposure, the surface area significantly lessened, as expected according to SEM images. This result can be addressed by the surface coverage and the partial blockage of the sludge pores and channels by the loading of Cr(VI) during the adsorption process, as evidenced by SEM images. This finding is another evidence for Cr adsorption onto the sludge surface.

Moreover, FTIR spectroscopy was used to detect the presence of functional groups on the fresh and spent biosorbent surface and the results are illustrated in Fig. 2. The vibration frequency peaks at about 470–900; 1,114; 1,385; 1,640; 2,400; 2,920 and 3,443 cm^{-1} can be recognized from the FTIR spectra of biosorbent before exposure to the effluent. The intense peaks at around 3,443 and 1,640 cm^{-1} characterize the stretching vibrations of bridging hydroxyl groups (O–H) and of carbonyl groups (C=O), respectively. The peak located at 1,114 cm^{-1} corresponds to aliphatic ether (C–O–C) stretching. The weak absorption peak at 1,385 cm^{-1} was confidently assigned to the C–O–H stretching of carboxylate anion. Moreover, the absorption bands appearing around 2,920 and 2,400 may be assigned to the C–H stretching vibrations in alkane or alkene groups and the C–O asymmetric stretching frequency, respectively. Based on the literature assignments, metal-oxygen stretching frequencies appear in the range of 470–900 cm^{-1} [40,41]. The FTIR results indicate that the surface of fresh biosorbent contains rich oxygen functional groups such as –CO, –COOH, –C=O and –OH. After exposure, the FTIR spectrum of the biosorbent depicts slight shifts in the position of the absorption bands, which indicates the oxygen functional groups such as hydroxyl and aliphatic ether may participate in the adsorption process. Besides, the new absorption band around 500–600 cm^{-1} can be detected over the FTIR spectrum of the spent adsorbent. This evidences the stretching vibration adsorption spectrum of Cr-O [42]. Accordingly, the occurrence of a slight shift in the peaks position and the presence of Cr-O vibration confirm the loading of Cr ions on the adsorbent structure.

As well known, the biosorption onto an adsorbent is affected by its pH_{PZC} [43]. Fig. 3 shows the point of zero charge determined by the salt addition method. The value obtained at the intersection of the initial pH (pH_0, *x*-axis) with the pH = 0 line (*y*-axis) gives the pH_{PZC}. As can be

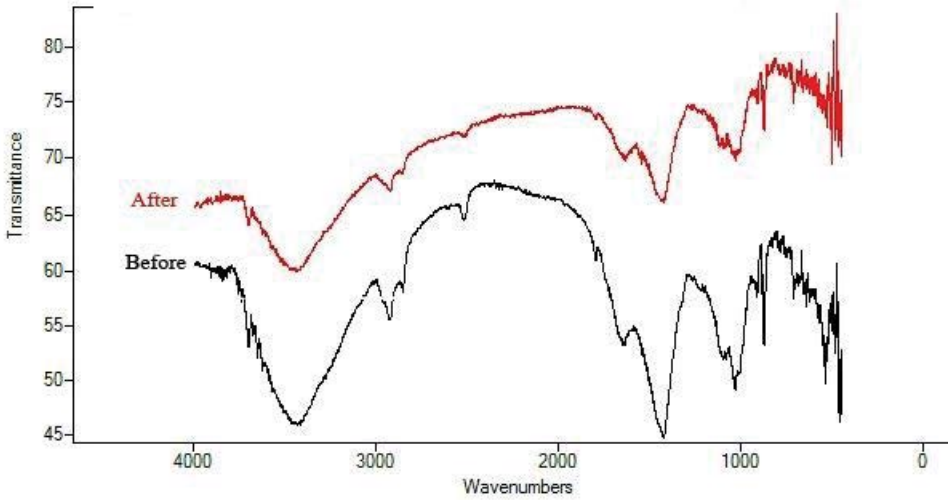

Fig. 2. FTIR analysis of the sludge before use (black) and after use (red) in Cr(VI) biosorption process.

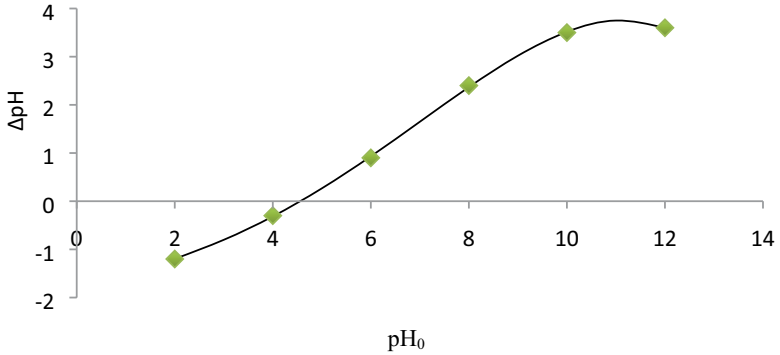

Fig. 3. ΔpH against initial pH for dried sludge sample at 25°C.

seen, the pH_{PZC} value determined is approximately 5. Therefore, the surface charge of the biosorbent close to this point is neutral. It was also found that the number of negatively charged sites on the biosorbent surface is more at pH_{PZC} < pH whereas, at pH below pH_{PZC}, the surface will have more positively charged functional groups. Since one of the mechanisms responsible for Cr adsorption on the surface is electrostatic attraction/repulsion, the charge of the surface can affect the Cr removal.

3.2. Effect of contact time

To determine the effect of contact time on Cr(VI) removal efficiency, the experiments were carried out at different times using a constant Cr(VI) concentration of 50 mg/L, a biosorbent dosage of 2 g/L and a pH of 5. The obtained results are shown in Fig. 4a. Statistical analysis also showed a significant relationship between time and Cr(VI) removal efficiency (p-value = 0.002). As can be seen, the removal efficiency rapidly increases within the initial 80 min, which is ascribed to greater contaminant concentration and more availability of vacant sorption sites on the adsorbent surface. Afterwards, the receptor sites are occupied and mass transfer driving force becomes weaker as a result of intraparticle diffusion effects and the decrease of contaminant concentration. This occurrence results in the gradual increase in the removal efficiency with the lapse of time until the adsorption equilibrium reaches, which is almost 100 min. afterwards, the removal efficiency remains constant. This can be attributed to the fact that all the available adsorbing sites on the surface of adsorbent are saturated and further adsorption is not possible [44,45].

3.3. Effect of biosorbent dosage

Fig. 4b illustrates the system performance changes in the removal of Cr(VI) under constant conditions (initial concentration of 50 mg/L, the optimum time of 100 min and pH of 5). As can be seen, the increase in biosorbent dosage primarily increases the Cr(VI) biosorption efficiency, which can be due to an increase in biosorption sites at the biosorbent surface [46]; but, at concentrations above 8 g/L, a slight decrease in system performance is visible because the biosorbent, after a while, reaches its maximum capacity in biosorption Cr(VI), and an increase beyond this level does not have a specific effect on the Cr(VI) biosorption efficiency [47]. Hereupon, the biosorbent dosage of 8 g/L was selected as the optimum value. Although the statistical analysis does not show a significant relationship between these two parameters (p-value = 0.081). This study is consistent

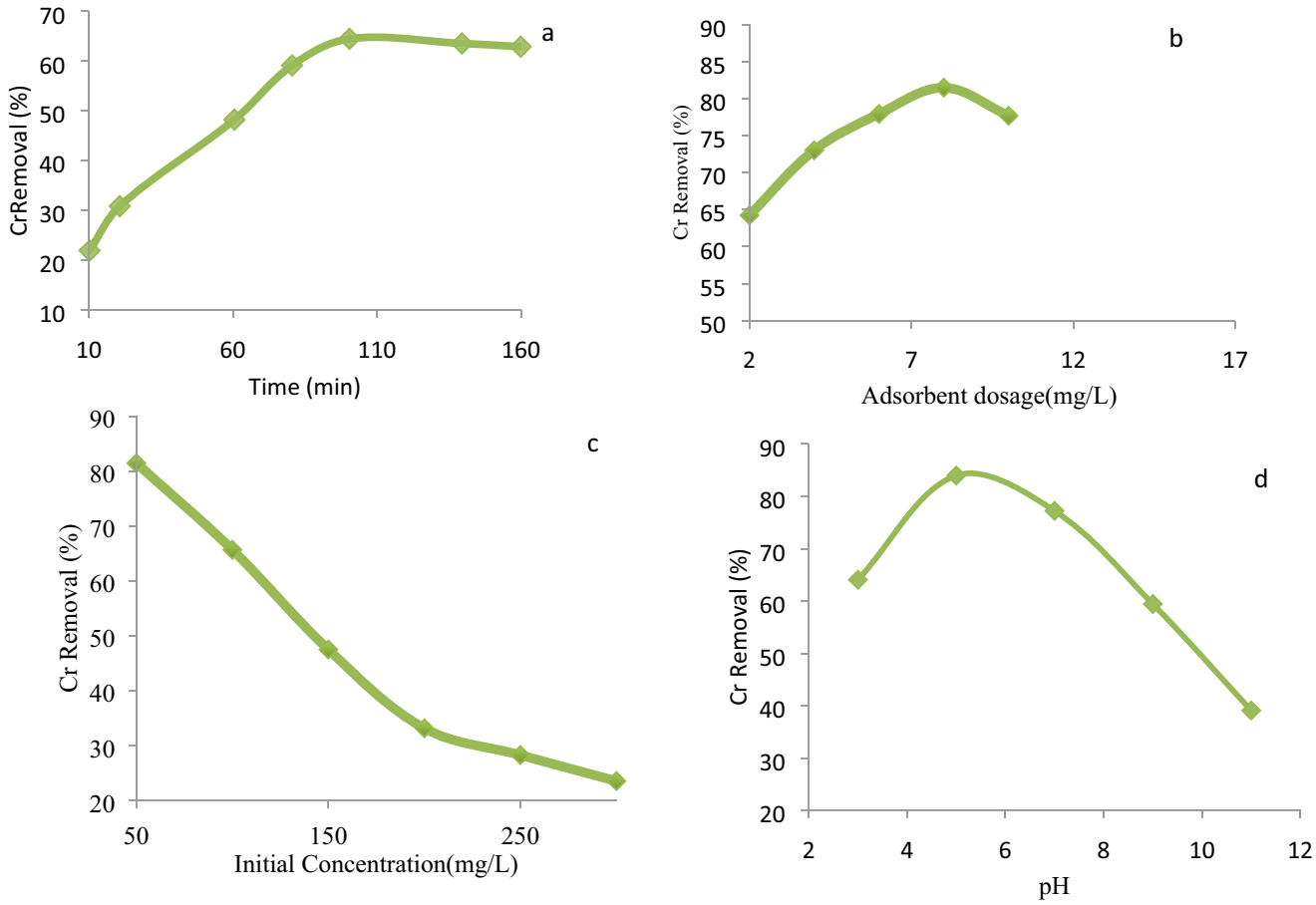

Fig. 4. (a) Effect of parameters including contact time, (b) adsorbent dose, (c) initial concentration of chromium and (d) pH on the adsorption of chromium metal.

with the research by Zare et al. [26] who has investigated the ability of dried sludge in the removal of Cu.

3.4. Effect of initial Cr(VI) concentration

To investigate the effect of Cr(VI) concentration on biosorption efficiency, the experiments conducted using initial Cr(VI) concentrations in the range of 50–200 mg/L under constant conditions of other effective parameters (time of 100 min, biosorbent dosage of 8 g/L and pH of 5). The results show that increasing the initial concentration would reduce the system efficiency from 81.46% to 54.23% (Fig. 4c). Thus, the initial concentration of 50 mg/L was selected as the optimum amount. Statistical analysis also showed a significant relationship between initial Cr(VI) concentration and its biosorption efficiency (p-value = 0.021). Similar results were observed in many other studies that have been used in the biosorption process. One of the reasons for this phenomenon is that, by increasing Cr(VI) concentration, active sites on the biosorbent are occupied, and the further biosorption of Cr(VI) is subject to an increase in time or an increase in biosorbent dosage. With further increase in Cr(VI) concentration, the active surface of the biosorbent is completely limited, hence the biosorption efficiency is reduced [45].

3.5. Effect of pH

As well known, the pH of the aqueous solution is one of the most important parameters in sorption process optimization. It affects not only the speciation of ions to be removed but also the availability of sorption sites. To assess the effect of initial pH on the Cr(IV) biosorption, the pH was changed in the range of 3–11 and other parameters were remained constant (at the initial concentration of 50 mg/L, time of 100 min and biosorbent dosage of 8 g/L). The results shown in Fig. 4d indicate that Cr removal is highly pH-dependent. As can be seen, the removal efficiency of total Cr increases from 64.07% to 83.96% while pH increases from 3 to 5. Then, the removal efficiency significantly declines to 39.11% with more increase in pH up to 11. Therefore, the pH value of 5.0 seems to be the optimal pH for Cr removal. Statistical analysis also showed the existence of a significant relationship (p-value = 0.005). The same trend of pH effect on Cr removal by biomaterials was reported in the literature [48,49]. The observed behavior of Cr sorption at various pH values is a consequence of electrostatic attraction/repulsion between the charged adsorbent surface and the oxy-anions of chromium. Based on the literature [49], the most prevalent species of Cr(VI) in solution are chromic acid (H_2CrO_4), acid chromate ($HCrO_4^-$), chromate (CrO_4^{2-}) and dichromate ($Cr_2O_7^{2-}$) which their stability depends upon the pH of the solution. The biosorbent is not able to adsorb at low pHs (1–6), $HCrO_4^-$ species are dominant which are gradually replaced by CrO_4^{2-} ions as the pH of the solution increases (above pH 6). At pH below pH_{PZC}, the biosorbent surface is positively charged due to protonation of the surface groups which favors the high biosorption efficiency of negatively charged Cr(VI) ions through strong electrostatic attraction. However, the acidic pH accelerates the reduction of Cr(VI) to Cr(III), resulting in a decrease of Cr(VI) anionic species in the solution. The following reduction reaction occurs in an acidic medium:

$$HCrO_4^- + 7H^+ + 3e^- \leftrightarrow Cr^{3+} + 4H_2O \quad (14)$$

$$Cr_2O_7^{2-} + 14H^+ + 6e^- \leftrightarrow 2Cr^{3+} + 7H_2O \quad (15)$$

Moreover, the affinity of the surface for Cr(III) sorption would be limited as the surface is protonated because of the charge repulsion between the cation and adsorbent surface. This reduces the likelihood of removal of total Cr at lower pHs. Accordingly, the increase of the adsorption efficiency by increasing the pH from 3 to 5 could be attributed to more availability of Cr(VI) anionic species and more surface affinity for Cr(III) despite a lesser degree of the biomass protonation which may occur. Above the point of zero charge ($>pH_{PZC}$), the sorption sites are deprotonated and the adsorbent surface is negatively charged. As pH increases beyond 5, the electrostatic repulsion between the adsorbent and negative chromate anions significantly increases, thereby reducing the removal efficiency. The induced competition between the OH^- ions with Cr(VI) species (CrO_4^{2-}) for sorption sites and the formation of insoluble heavy metal hydroxides such as $Cr(OH)_3$ at higher pHs may be other reasons for the reduction in uptake of Cr(VI) ions.

3.6. Biosorption isotherms

The isotherm of adsorption indicates how the quantities of molecules are distributed between the liquid and solid phase when the adsorption processes reach balance [50]. It is employed to establish the maximum capacity of chromium adsorption on biosorbent. Fig. 5 shows the experimental and the predicted two and three-parameter isotherms for the chromium adsorption onto prepared biosorbent. The parameters of the six isotherm models studied are also represented in Table 3.

The Langmuir isotherm (R^2 = 0.9984) and Redlich–Peterson isotherm (R^2 = 0.9993) have almost the same and high coefficient of determination when compared to other isotherms (Table 3). On the other hand, the g parameter in Redlich–Peterson isotherm is nearly unity, this indicated that the equilibrium isotherm is approaching the Langmuir but not the Freundlich isotherm.

In the Langmuir isotherm, it is assumed that biosorption occurs in a series of homogeneous sites inside the biosorbent [51]. The dimensionless constant separation factor (R_L) is also used to test the applicability of the Langmuir equation and is expressed as Eq. (16):

$$R_L = \frac{1}{1 + bC_0} \quad (16)$$

where C_0 is the initial concentration of the solution and b is the Langmuir constant. If the $R_L > 1$, the use of the model is unfavorable; if $R_L = 1$, the use of the linear model is appropriate; if $0 < R_L < 1$, the model is appropriate and if $R_L = 0$, the model is inefficient [52]. The results show that in all cases, R_L values were between 0 and 1 (at a range of 0.03–0.35).

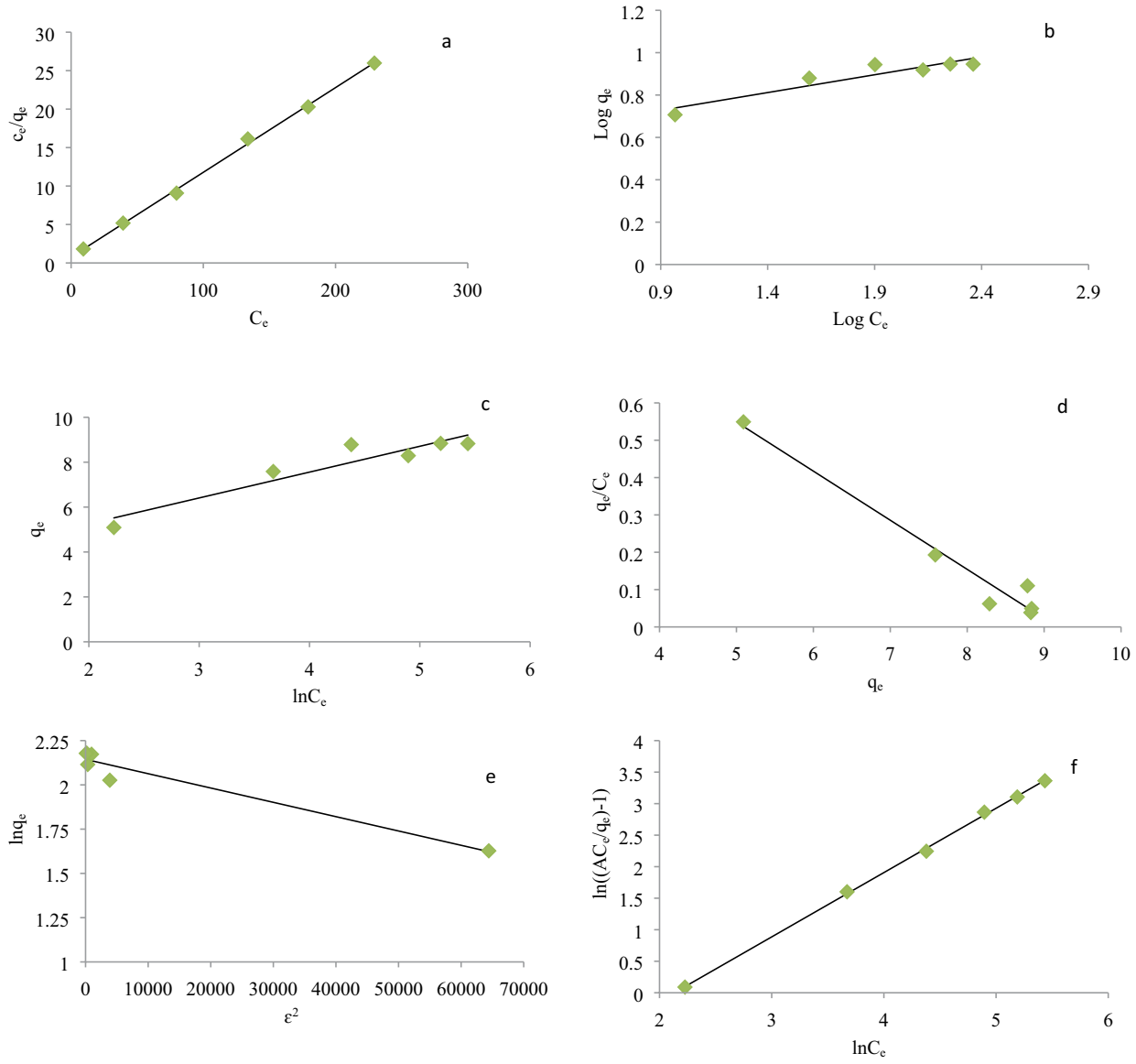

Fig. 5. (a) Langmuir, (b) Freundlich, (c) Temkin, (d) Scatchard, (e) Dubinin–Radushkevich and (f) Redlich–Peterson models in Cr(VI) biosorption process.

It can be concluded that chromium removal occurs on a biosorbent with the homogenous surface by monolayer adsorption and all of the adsorption sites are equally probable. It can be described in terms of chemisorption (limited to a monolayer) as the formation of the strong attractive interaction between adsorbate and adsorbent, but weak interaction between the adsorbate themselves. This is confirmed by the coefficient of determination. Consequently, the Langmuir isotherm and especially, three-parameter Redlich–Peterson isotherm found to be the most suitable models for this biosorption system compared with other isotherms.

3.7. Biosorption kinetics

The rate or kinetics of biosorption is used to understand the dynamics of biosorption reactions, which is applied to determine and select the optimum conditions for full-scale operation [53].

In this study, the kinetics models, that is, pseudo-first-order, pseudo-second-order, and intra-particle diffusion were investigated for Cr(VI) biosorption under optimal conditions at different times (Table 4). The results are shown in Fig. 6. Regarding the obtained constant and correlation coefficients, the process follows the pseudo-second-order kinetic model. Hence, chemical biosorption has been a limiting step in the biosorption process, which results obtained from the isotherm of the process also confirm this claim. This result is consistent with similar studies in the removal of Cr(VI) [54,55]. The half-life ($t_{1/2}$) of Cr(VI) was obtained as 0.67 h. The short half-life for the sorption process indicates that the Cr(VI) biosorption process occurs fast and Cr(VI) biosorption directly depends on the biosorption

Table 3
The obtained parameters of isotherms in Cr(VI) biosorption process

Isotherm		Linear form	Parameters	
Langmuir	$q_e = \frac{q_m k_1 C_e}{1 + k_1 C_e}$	$\frac{C_e}{q_e} = \frac{1}{k_1 q_m} + \frac{C_e}{q_m}$	q_m (mg/g)	9.0826
			k_1 (L/mg)	0.1425
			R^2	0.9984
			R_L	0.03–0.35
Freundlich	$q_e = K_F C_e^{\frac{1}{n}}$	$\log q_e = \log K_F + \frac{1}{n}\log C_e$	n	5.9488
			K_F (mg/g)(L/mg)$^{1/n}$	3.7696
			R^2	0.8712
Temkin	$q_e = \frac{RT}{b}\ln\left(AC_e\right)$	$q_e = B\ln A_T + B\ln C_e$	A_T (L/g)	5.8561
			B (J/mol)	1.3375
			R^2	0.8930
Scatchard	$\frac{q_e}{C_e} = K_s\left(Q_s - q_e\right)$	$\frac{q_e}{C_e} = Q_s K_s - q_e K_s$	Q_s	9.1687
			K_s	0.1316
			R^2	0.964
Dubinin–Radushkevich	$q_e = q_m \exp\left(-\beta\varepsilon^2\right)$	$\ln q_e = \ln q_m - \beta\varepsilon^2$	q_m (mg/g)	8.5335
			β (mol^2/J^2)	8 × 10^{-6}
			R^2	0.9478
			E (kJ/mol)	0.25
Redlich–Peterson	$q_e = \frac{AC_e}{1 + BC_e^g}$	$\ln\left[A\frac{C_e}{q_e} - 1\right] = g\ln C_e + \ln B$	g	0.9995
			B (L/mg)	0.1374
			A (L/g)	1.15
			R^2	0.9993

Table 4
Kinetics parameters for the adsorption of Cr(VI) onto dried activated sludge

$q_{e,\text{exp.}}$ (mg/g)	Pseudo-first-order			Pseudo-second-order			Intraparticle diffusion		
	$q_{e,\text{cal.}}$ (mg/g)	k_1 (min^{-1})	R^2	$q_{e,\text{cal.}}$ (mg/g)	k_2 (g mg^{-1} min^{-1})	R^2	k_{diff} (mg g^{-1} min$^{1/2}$)	c	R^2
9.082	81.77	9.2 × 10^{-4}	0.9878	9.67	1.8 × 10^{-3}	0.9973	0.0756	2.78	0.9859

capacity and inversely relates to the initial biosorption rate [56].

3.8. Efficiency of the biosorbent in removal of Cr(VI) from the real wastewater

To determine the Cr(VI) removal efficiency in real wastewater, four real samples were taken from electroplating industries. The characteristics of real electroplating industries effluent samples are shown in Table 2. Real wastewater samples were examined to determine the Cr(VI) biosorption efficiency under optimum conditions (time = 100 min, biosorbent dosage = 8 g/L and pH = 5). The results showed that by increasing the initial concentration of Cr(VI) and pH values, the biosorption efficiency was decreased, which is also consistent with the obtained results (Fig. 7).

Furthermore, the biosorption efficiency in the real wastewater was lower than that of synthetic wastewaters, which could be due to the probability of the presence of other compounds and heavy metals in the real wastewater. Indeed, the existence of different compounds in the real effluents acts as a competitive factor with the biosorption of Cr(VI) and reduces the biosorption of Cr(VI) by occupying the biosorbent sites [57].

3.9. Thermodynamics for adsorption

The process of Cr adsorption can be represented by the reversible process between Cr species in the solution and ones onto the adsorbent surface, which represents a heterogeneous equilibrium. To investigate the thermodynamic behavior of the Cr adsorption onto prepared biosorbent, Gibbs free energy change ($\Delta G°$) was determined using the following equation:

$$\Delta G° = -RT\ln K_{\text{eq}} \tag{17}$$

where R (8.314 J/mol K) is the universal gas constant, T (K) is the absolute temperature, and K_{eq} is the adsorption equilibrium constant which is defined as follows:

$$K_{\text{eq}} = \frac{C_a}{C_e} \tag{18}$$

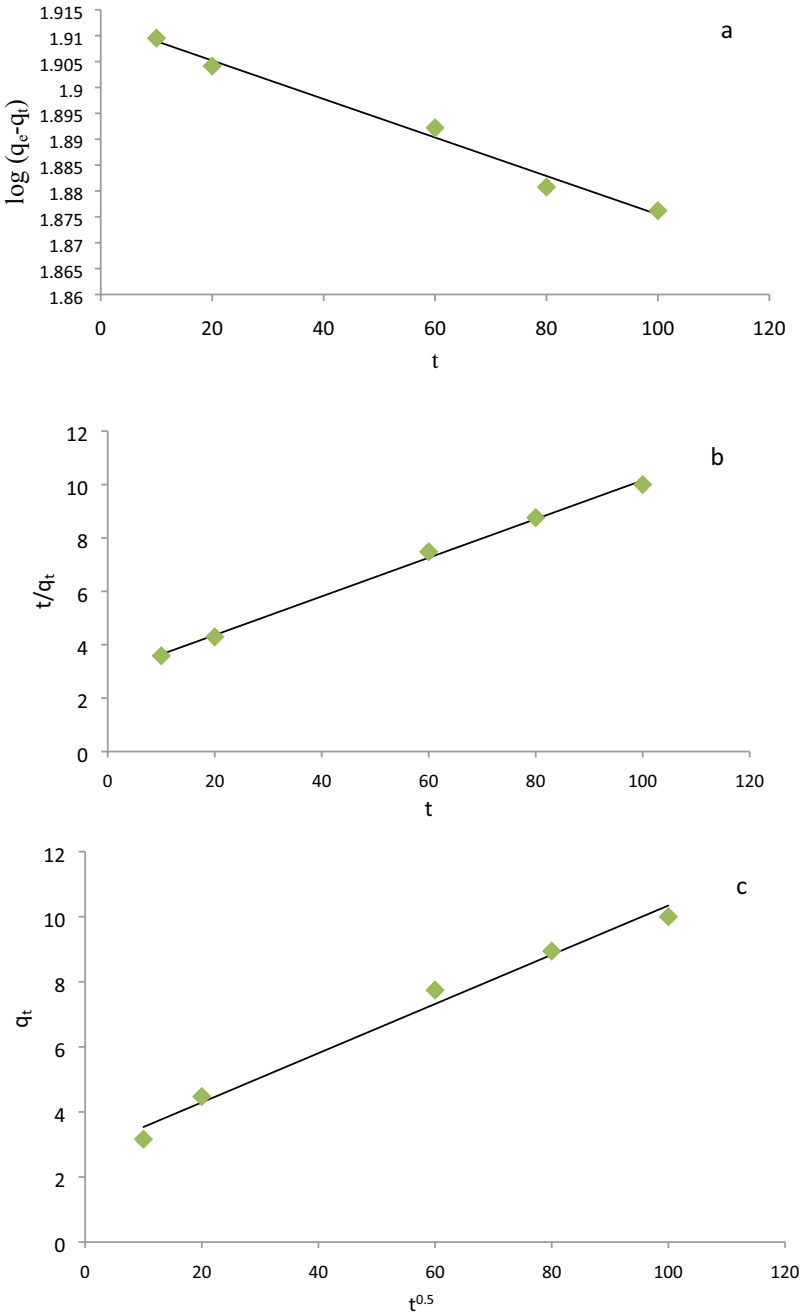

Fig. 6. Study of (a) pseudo-first-order, (b) pseudo-second-degree and (c) particle penetration under optimum conditions at different times.

where C_a is the equilibrium concentration of Cr onto the prepared biosorbent and C_e is the equilibrium concentrations of solute in the solution, respectively.

The Gibbs free energy indicates the degree of the spontaneity of the adsorption process, where more negative values reflect a more energetically favorable adsorption process. The value of $\Delta G°$ in this study (–3.67 kJ/mol) confirms the feasibility of biosorbent and the spontaneity of the adsorption process. The $\Delta G°$ for the prepared biosorbent shows that it has got a large capacity and affinity for the selective removal of Cr from aqueous solution.

3.10. Possible adsorption mechanism

The adsorption mechanism of chromium ions on prepared biosorbent may originate from the available functional groups and solution pH. When Cr(VI) oxyanions contact with surface functional groups appeared as confirmed by FTIR analysis (–COOH, –OH, –CO and C=O), reduction of Cr(VI) into Cr(III) takes place in aqueous medium duo to high redox potential value of Cr(VI) (1.3 V at standard state) in an acidic medium. The reduction of Cr(VI) oxyanions can be explained by the following two pathways: first, the

Table 5
Comparison of maximum adsorption capacity (q_{max}) for Cr(VI) with various new adsorbents

Adsorbent	Temperature (°C)	Dose (g/L)	q_{max} (mg/g)	Cr(VI) concentration (mg/L)	Time	References
Dried sludge	25	8.0	9.082	50	100 min	Present Study
Chitosan/clay/Fe_3O_4	25	1	97.08	10	30 min	[58]
Bentonite clay@$MnFe_2O_4$	25	1.5	178.6	10	60 min	[59]
MgO/Fe_3O_4	25	1.5	23.9	10	30 min	[60]
Ziziphus spina–christi leaf	60	5	13.81	10	55 min	[61]
Bentonite/biocoal	25	1	64.102	10	60 min	[62]
Activated carbon/$CoFe_2O_4$	25	1.5	70.42	10	60 min	[63]

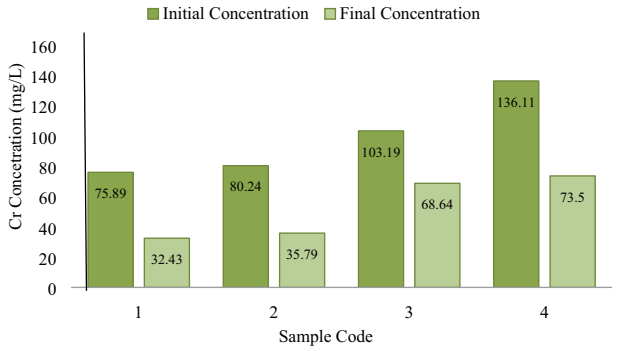

Fig. 7. Cr(VI) biosorption efficiency from the real electroplating industry wastewater under optimum conditions (contact time = 100 min; adsorbent dosage = 8 g/L; pH = 5).

reduction of Cr(VI) to Cr(III) in the presence carbonaceous compounds (C_xOH) as the main surface electron-donor groups of biosorbent in acidic medium (Eqs. (17) and (18)). As evidence from EDX analysis, carbon is one of the main components in the waste biomaterial and played a vital role in chromium species removal.

$$3C_xOH + Cr_2O_7^{2-} + 4H^+ \rightarrow 3C_xO + HCrO_4^- + Cr^{3+} + 3H_2O \quad (19)$$

$$3C_xOH + HCrO_4^- + 4H^+ \rightarrow 3C_xO + Cr^{3+} + 4H_2O \quad (20)$$

The second mechanism involves the interaction between negatively charged chromium species, and positively charged groups which protonated by H^+ ions in acidic medium and the biosorption coupled reduction of Cr(VI) to Cr(III) occurs on the adsorbent sites, according to Eqs. (17) and (18).

3.11. Comparison of Cr(VI) removal with different adsorbents reported in literature

To better evaluate and ensure the performance of the prepared biosorbent, the adsorption capacity was compared with other new adsorbents used in the literature. Table 5 illustrates different adsorbents examined in the removal of Cr(VI) under their optimal operation conditions. Adsorption capacity is an appropriate criterion to compare the results obtained to those investigated in the cited literature. However, it depends on the initial concentration of the adsorbate. Although the maximum adsorption capacity of the current investigation is lower than other new adsorbents, due to the low cost of bioabsorbent, easy preparation, the need for fewer chemicals and eco-friendly biosorbent, the biomass of dried sludge seems to have the appropriate performance towards Cr removal.

4. Conclusion

The main objective of the present study was to investigate the efficiency of Cr(VI) biosorption from aqueous solution and industrial effluent by biomass of dried sludge. The physicochemical properties of fresh and spent biosorbent derived from sludge were characterized and utilized in experiments. The characterization results of fresh biosorption showed a suitable surface area and the presence of a desirable functional group for biosorption. Furthermore, the porous structure of biosorbent confirmed by SEM analysis made it a perfect absorbent. The highest Cr(VI) biosorption efficiency was 83.96% at pH of 5, the contact time of 100 min, the initial concentration of 50 mg/L, and the biosorbent dosage of 8 g/L. The EDX and FTIR spectra of the spent adsorbent alongside the BET surface area and FESEM images confirmed the loading of Cr ions on the adsorbent structure. The obtained biosorption data agreed well with the pseudo-second-order model as well as it followed the Redlich–Peterson isotherm model with an R^2 value of 0.9993. The thermodynamic study by $\Delta G°$ value (–3.67 kJ/mol) indicated the feasibility and spontaneity of the biosorption process on daring sludge. Accordingly, the use of dried sludge, as a cheap and available biosorbent, can be used as an appropriate option in the removal of Cr(VI) from industrial wastewater. Moreover, further studies are suggested to investigate and to propose a suitable method for the disposal of produced sludge or recovery of adsorbed metal from the adsorbent.

Acknowledgment

The authors acknowledge Mashhad University of Medical Science and the University of Kurdistan for the financial support to make this research possible.

References

[1] S.-H. Liu, G.-M. Zeng, Q.-Y. Niu, Y. Liu, L. Zhou, L.-H. Jiang, X.-F. Tan, P. Xu, C. Zhang, M. Cheng, Bioremediation mechanisms of combined pollution of PAHs and heavy metals by bacteria and fungi: a mini review, Bioresour. Technol., 224 (2017) 25–33.

[2] S.M. Aghili, N. Mehrdadi, M.A. Zazouli, B. Aminzadeh, Heavy metal concentrations in dewatered sludge of wastewater treatment plant in Sari, Iran, J. Mazandaran Univ. Med. Sci., 28 (2019) 152–159.
[3] S. Tasharrofi, S.S. Hassani, H. Taghdisian, Z. Sobat, Chapter 24 – Environmentally Friendly Stabilized nZVI-Composite for Removal of Heavy Metals, C.M. Hussain, A.K. Mishra, Eds., New Polymer Nanocomposites for Environmental Remediation, Elsevier, 2018, pp. 623–642.
[4] Z. Esvandi, R. Foroutan, M. Mirjalili, G.A. Sorial, B. Ramavandi, Physicochemical behavior of *Penaeuse semisulcatuse* chitin for Pb and Cd removal from aqueous environment, J. Polym. Environ., 27 (2019) 263–274.
[5] M. Shafiee, R. Foroutan, K. Fouladi, M. Ahmadlouydarab, B. Ramavandi, S. Sahebi, Application of oak powder/Fe_3O_4 magnetic composite in toxic metals removal from aqueous solutions, Adv. Powder Technol., 30 (2019) 544–554.
[6] S. Abbasi, R. Foroutan, H. Esmaeili, F. Esmaeilzadeh, Preparation of activated carbon from worn tires for removal of Cu(II), Ni(II) and Co(II) ions from synthetic wastewater, Desal. Water Treat., 141 (2019) 269–278.
[7] B. Dovlati, E. Naderi, H. Pirkharrati, Kh. Farhadi, Removal of chromium (Cr^{3+}) and (Cr^{6+}) from aqueous solutions using leonardite, J. Water Wastewater, 30 (2019) 91–102.
[8] M.A. Hashem, M.A. Momen, M. Hasan, M.S. Nur-A-Tomal, M.H. Sheikh, Chromium removal from tannery wastewater using *Syzygium cumini* bark adsorbent, Int. J. Environ. Sci. Technol., 16 (2019) 1395–1404.
[9] M. Sharma, J. Singh, S. Hazra, S. Basu, Adsorption of heavy metal ions by mesoporous ZnO and TiO_2@ZnO monoliths: adsorption and kinetic studies, Microchem. J., 145 (2019) 105–112.
[10] S. Srivastava, S. Agrawal, M. Mondal, Biosorption isotherms and kinetics on removal of Cr(VI) using native and chemically modified *Lagerstroemia speciosa* bark, Ecol. Eng., 85 (2015) 56–66.
[11] S. Elabbas, L. Mandi, F. Berrekhis, M.N. Pons, J.P. Leclerc, N. Ouazzani, Removal of Cr(III) from chrome tanning wastewater by adsorption using two natural carbonaceous materials: eggshell and powdered marble, J. Environ. Manage., 166 (2016) 589–595.
[12] S. Gunatilake, Methods of removing heavy metals from industrial wastewater, J. Multidiscip. Eng. Sci. Stud., 1 (2015) 12–18.
[13] M. Haghighi, F. Rahmani, R. Dehghani, A.M. Tehrani, M.B. Miranzadeh, Photocatalytic reduction of Cr(VI) in aqueous solution over ZnO/HZSM-5 nanocomposite: optimization of ZnO loading and process conditions, Desal. Water Treat., 58 (2017) 168–180.
[14] F. Minas, B.S. Chandravanshi, S. Leta, Chemical precipitation method for chromium removal and its recovery from tannery wastewater in Ethiopia, Chem. Int., 3 (2017) 392–405.
[15] M.K.N. Mahmad, M.M.R. Rozainy, I. Abustan, N. Baharun, Electrocoagulation process by using aluminum and stainless steel electrodes to treat total chromium, color and turbidity, Procedia Chem., 19 (2016) 681–686.
[16] M. Jyothi, V. Nayak, M. Padaki, R.G. Balakrishna, K. Soontarapa, Eco-friendly membrane process and product development for complete elimination of chromium toxicity in wastewater, J. Hazard. Mater., 332 (2017) 112–123.
[17] G. Vilardi, J.M. Ochando-Pulido, N. Verdone, M. Stoller, L. Di Palma, On the removal of hexavalent chromium by olive stones coated by iron-based nanoparticles: equilibrium study and chromium recovery, J. Cleaner Prod., 190 (2018) 200–210.
[18] D.M. Angelucci, V. Stazi, A.J. Daugulis, M.C. Tomei, Treatment of synthetic tannery wastewater in a continuous two-phase partitioning bioreactor: biodegradation of the organic fraction and chromium separation, J. Cleaner Prod., 152 (2017) 321–329.
[19] M. Haghighi, F. Rahmani, F. Kariminejad, R.A. Sene, Photodegradation of lignin from pulp and paper mill effluent using TiO_2/PS composite under UV-LED radiation: optimization, toxicity assessment and reusability study, Process. Saf. Environ. Prot., 122 (2019) 48–57.
[20] Z. Yousefi, J. Yazdani Cherati, M. Movahedi, F. Kariminejad, Effect of organic loading rate on the performance of anaerobic process in treatment of pulp and paper mill effluents, J. Mazandaran Univ. Med. Sci., 25 (2015) 136–150.
[21] M.R. Rahimzadeh, S. Kazemi, A.A. Moghadamnia, Cadmium toxicity and treatment: an update, Caspian J. Int. Med., 8 (2017) 135.
[22] S. Guiza, Biosorption of heavy metal from aqueous solution using cellulosic waste orange peel, Ecol. Eng., 99 (2017) 134–140.
[23] F. Kariminejad, Z. Yousefi, J.Y. Cherati, Evaluation of COD, color and lignin removal from pulp and paper effluent by anaerobic sludge biosorption, Int. J. Environ. Sci. Technol., 15 (2018) 719–732.
[24] A. Witek Krowiak, R.G. Szafran, S. Modelski, Biosorption of heavy metals from aqueous solutions onto peanut shell as a low-cost biosorbent, Desalination, 265 (2011) 126–134.
[25] A. Rezgui, Y. Hannachi, E. Guibal, T. Boubaker, Biosorption of zinc from aqueous solution by dried activated sludge biomass, Desal. Water Treat., 56 (2015) 2699–2705.
[26] H. Zare, H. Heydarzade, M. Rahimnejad, A. Tardast, M. Seyfi, Dried activated sludge as an appropriate biosorbent for removal of copper(II) ions, Arabian J. Chem., 8 (2015) 858–864.
[27] O. Gulnaz, A. Kaya, S. Dincer, The reuse of dried activated sludge for adsorption of reactive dye, J. Hazard. Mater., 134 (2006) 190–196.
[28] A. Maleki, A.H. Mahvi, M.A. Zazouli, H. Izanloo, A.H. Barati, Aqueous cadmium removal by adsorption on barley hull and barley hull ash, Asian J. Chem., 23 (2011) 1373–1376.
[29] M.A. Zazouli, P. Ebrahimi, M. Bagheri Ardebilian, Study of Cd(II) and Cr(VI) biosorption by mesocarps of orange and sour orange from aqueous solutions, Environ. Eng. Manage. J., 13 (2014) 345–351.
[30] H. Demey, T. Vincent, E. Guibal, A novel algal-based sorbent for heavy metal removal, Chem. Eng. J., 332 (2018) 582–595.
[31] Z. Rahman, L. Thomas, V.P. Singh, Biosorption of heavy metals by a lead (Pb) resistant bacterium, *Staphylococcus hominis* strain AMB-2, J. Basic Microbiol., 59 (2019) 477–486.
[32] W. Boulaiche, B. Hamdi, M. Trari, Removal of heavy metals by chitin: equilibrium, kinetic and thermodynamic studies, Appl. Water Sci., 9 (2019) 39, https://doi.org/10.1007/s13201-019-0926-8.
[33] B.P. Zhang, X.L. Han, P.J. Gu, S.Q. Fang, J. Bai, Response surface methodology approach for optimization of ciprofloxacin adsorption using activated carbon derived from the residue of desilicated rice husk, J. Mol. Liq., 238 (2017) 316–325.
[34] P. Javanmardi, A. Takdastan, R. Jalilzadeh, M.J. Mohammadi, Study the efficiency and effective factors on the application of clinoptilolite zeolite for removal of Zn from aqueous solutions, determination of the adsorption kinetics and isotherms, J. Environ. Health Eng., 4 (2016) 43–57.
[35] R. Foroutan, R. Mohammadi, A.S. Adeleye, S. Farjadfard, Z. Esvandi, H. Arfaeinia, G.A. Sorial, B. Ramavandi, S. Sahebi, Efficient arsenic(V) removal from contaminated water using natural clay and clay composite adsorbents, Environ. Sci. Pollut. Res., 26 (2019) 29748–29762.
[36] R. Foroutan, R. Mohammadi, N. Sohrabi, S. Sahebi, S. Farjadfard, Z. Esvandi, B. Ramavandi, Calcined alluvium of agricultural streams as a recyclable and cleaning tool for cationic dye removal from aqueous media, Environ. Technol. Innov., 17 (2020) 100530.
[37] M.M. Boushehrian, H. Esmaeili, R. Foroutan, Ultrasonic assisted synthesis of Kaolin/$CuFe_2O_4$ nanocomposite for removing cationic dyes from aqueous media, J. Environ. Chem. Eng., 8 (2020) 103869.
[38] A. Farhan, K. Ong, W.W. Yunus, M. Jabit, A. Fitrianto, A. Hussin, A. Sulaiman, S. Jamal, J. Osman, C. Teoh, Kinetics study of nickel(II) ions sorption by thermally treated rice husk, Nat. Environ. Pollut. Technol., 16 (2017) 889.
[39] R. Foroutan, R. Mohammadi, S. Farjadfard, H. Esmaeili, B. Ramavandi, G.A. Sorial, Eggshell nano-particle potential for methyl violet and mercury ion removal: surface study and field application, Adv. Powder Technol., 30 (2019) 2188–2199.

[40] P. Delir Kheyrollahi Nezhad, M. Haghighi, F. Rahmani, CO_2/O_2-enhanced ethane dehydrogenation over a sol–gel synthesized Ni/ZrO_2–MgO nanocatalyst: effects of Mgo, ZrO_2, and NiO on the catalytic performance, Part. Sci. Technol., 36 (2018) 1017–1028.
[41] A. Talati, M. Haghighi, F. Rahmani, Oxidative dehydrogenation of ethane to ethylene by carbon dioxide over Cr/TiO_2–ZrO_2 nanocatalyst: effect of active phase and support composition on catalytic properties and performance, Adv. Powder Technol., 27 (2016) 1195–1206.
[42] F. Rahmani, M. Haghighi, One-pot hydrothermal synthesis of ZSM-5–CeO_2 composite as a support for Cr-based nanocatalysts: influence of ceria loading and process conditions on CO_2-enhanced dehydrogenation of ethane, RSC Adv., 6 (2016) 89551–89563.
[43] M. Roushani, Z. Saedi, Y.M. Baghelani, Removal of cadmium ions from aqueous solutions using TMU-16-NH_2 metal organic framework, Environ. Nanotechnol. Monit. Manage., 7 (2017) 89–96.
[44] L. Ramrakhiani, A. Halder, A. Mandal, S. Majumdar, S. Ghosh, Toxic Metal Removal Using Biosorption Process and Inertization of Generated Hazardous Metal-Laden Biosorbent, S.K. Ghosh, Ed., Utilization and Management of Bioresources, Springer, Singapore, 2018, pp. 301–311.
[45] R. Shokohi, S.H. Sadeghi, K. Karimian, M.H. Saghi, Removal of acid cyanine 5R dye by surface biosorption process using dried activated sludge, J. Environ. Health Eng., 2 (2014) 108–118.
[46] E. Giarratano, M. Faleschini, C. Bruni, N.L. Olivera, M.N. Gil, Metal removal from wastewater using sludge from a natural stabilization pond as biosorbent, Int. J. Environ. Res., 13 (2019) 581–595.
[47] S. Hojati, A. Landi, Kinetic and thermodynamic studies of zinc removal from a metal-plating wastewater using Firouzkouh zeolite, J. Environ. Stud., 40 (2015) 901–912.
[48] R.M. Kulkarni, K. Vidya Shetty, G. Srinikethan, Kinetic and equilibrium modeling of biosorption of nickel(II) and cadmium(II) on brewery sludge, Water Sci. Technol., 79 (2019) 888–894.
[49] M. Samarghandi, S. Azizian, M. Shirzad Siboni, Removal of hexavalent chromium from aqueous solution by modified holly sawdust: a study of equilibrium and kinetics scientific, J. Hamadan Univ. Med. Sci., 16 (2010) 61–67.
[50] M. Malakootian, K. Yaghmaeian, R. Momenzadeh, Performance evaluation of adsorbent leca–modified (TiO_2/LECA) for the removal of anionic surfactants from wastewater, J. Knowl. Health, 11 (2016) 41–48.
[51] J.S. He, J.P. Chen, A comprehensive review on biosorption of heavy metals by algal biomass: materials, performances, chemistry, and modeling simulation tools, Bioresour. Technol., 160 (2014) 67–780.
[52] A.T.A. Farhan, K.K. Ong, W.M.Z. WanYunus, M.L. Jabit, A.G.A. Fitrianto, A. Hussin, C.C. Teoh, Isotherm study of nickel(II) adsorption from aqueous solution using thermally treated rice husk, Asian J. Chem., 29 (2017) 589–591.
[53] M. Malakootian, N. Yousefi, H.N. Jaafarzadeh, Kinetics modeling and isotherms for adsorption of phosphate from aqueous solution by modified clinoptilolite, J. Water Wastewater, 4 (2011) 21–29.
[54] M. Farrokhi, M. Shirzad Siboni, S. Tajasosi, M. Naeimi Jobeini, Removal of hexavalent chromium Cr(VI) from aqueous solution using adsorption onto modified alder sawdust: a study of equilibrium and kinetics, J. Guilan Univ. Med. Sci., 23 (2014) 57–65.
[55] A. Rahmani, R. Noorozi, M.T. Samadi, M. Shirzad Siboni, Removal of hexavalent chromium from aqueous solution by using adsorption onto commerical iron powder study of equilibrium and kinetics scientific, J. Hamadan Univ. Med. Sci., 18 (2011) 33–39.
[56] M. Sahmoune, K. Louhab, A. Boukhiar, Biosorption of Cr(III) from aqueous solutions using bacterium biomass *Streptomyces rimosus*, Int. J. Environ. Res., 3 (2009) 229–238.
[57] E. Pajootan, M. Arami, N.M. Mahmoodi, Binary system dye removal by electrocoagulation from synthetic and real colored wastewaters, J. Taiwan Inst. Chem. Eng., 43 (2012) 283–290.
[58] R. Foroutan, S.J. Peighambardoust, R. Mohammadi, M. Omidvar, G.A. Sorial, B. Ramavandi, Influence of chitosan and magnetic iron nanoparticles on chromium adsorption behavior of natural clay: adaptive neuro-fuzzy inference modeling, Int. J. Biol. Macromol., 151 (2020) 355–365.
[59] A. Ahmadi, R. Foroutan, H. Esmaeili, S. Tamjidi, The role of bentonite clay and bentonite clay@$MnFe_2O_4$ composite and their physico-chemical properties on the removal of Cr(III) and Cr(VI) from aqueous media, Environ. Sci. Pollut. Res., 27 (2020) 14044–14057.
[60] Y. Abshirini, H. Esmaeili, R. Foroutan, Enhancement removal of Cr(VI) ion using magnetically modified MgO nanoparticles, Mater. Res. Express, 6 (2019) 125513.
[61] Y. Abshirini, R. Foroutan, H. Esmaeili, Cr(VI) removal from aqueous solution using activated carbon prepared from *Ziziphus spina*–christi leaf, Mater. Res. Express, 6 (2019) 045607.
[62] R. Foroutan, R. Zareipour, R. Mohammadi, Fast adsorption of chromium(VI) ions from synthetic sewage using bentonite and bentonite/bio-coal composite: a comparative study, Mater. Res. Express, 6 (2018) 025508.
[63] R. Foroutan, R. Mohammadi, B. Ramavandi, M. Bastanian, Removal characteristics of chromium by activated carbon/$CoFe_2O_4$ magnetic composite and *Phoenix dactylifera* stone carbon, Korean J. Chem. Eng., 35 (2018) 2207–22019.